https://doi.org/10.17221/104/2024-CJGPB

High levels of type II Fusarium head blight resistance conferred in wheat by combining wheat gene *Fhb1* with *Lophopyrum elongatum* gene *Fhb7^{The2}*

Jan Dvorak[1], Karin R. Deal[1], Patrick E. McGuire[1], Emily J. Conley[2], James A. Anderson[2], George Fedak[3], Julia A. Malvick[4], Han Chen[5], Hans-Georg Müller[5]*

[1]*Department of Plant Sciences, University of California, Davis, USA*
[2]*Department of Agronomy and Plant Genetics, University of Minnesota, St. Paul, USA*
[3]*Ottawa Research and Development Center, Agriculture and Agri-Food Canada, Ottawa, Canada*
[4]*Veterinary Genetics Laboratory, University of California, Davis, USA*
[5]*Department of Statistics, University of California, Davis, USA*

**Corresponding author: jdvorak@ucdavis.edu*

Citation: Dvorak J., Deal K.R., McGuire P.E., Conley E.J., Anderson J.A., Fedak G., Malvick J.A., Chen H., Müller H.G. (2025): High levels of type II Fusarium head blight resistance conferred in wheat by combining wheat gene *Fhb1* with *Lophopyrum elongatum* gene *Fhb7^{The2}*. Czech J. Genet. Plant Breed., 61: 31–42.

Abstract: Wheat Fusarium head blight (FHB) leads to losses of grain yield and quality. Ingestion of diseased grain is detrimental to human health due to the mycotoxins present in the grain. Developing resistant cultivars for environments where FHB is prevalent is therefore an important breeding objective. One of the most effective wheat genes conferring type II resistance to FHB is *Fhb1,* originally discovered in the Chinese cultivar (cv) Sumai 3. Another excellent FHB resistance gene is *Fhb7* located on the long arm of *Lophopyrum elongatum* chromosome 7E. Several alleles of *Fhb7* have been identified. Allele *Fhb7^{The2}* was found in disomic substitution lines 7E(7A), 7E(7B) and 7E(7D) derived from amphiploid AgCS. The amphiploid was produced from a hybrid *Triticum aestivum* cv Chinese Spring × *L. elongatum*. To find if combining *Fhb7^{The2}* with *Fhb1* confers higher resistance in wheat than single genes, an introgression line derived from AgCS and possessing *Fhb7^{The2}* was recurrently backcrossed to bread wheat cv Rollag and MN-Washburn possessing *Fhb1.* Experimental lines possessing both *Fhb7^{The2}* and *Fhb1* were developed and validated cytogenetically and with the *L. elongatum* genome-wide Sequenom SNP MassARRAY. Spikes of these lines, parental cv Rollag and MN-Washburn, and those of disomic addition line 7E possessing *Fhb7^{The2}* plus controls were inoculated with Fusarium in a twice-replicated trial in controlled greenhouse environmental conditions. FHB infection rates were significantly lower in lines combining *Fhb7^{The2}* with *Fhb1* than in materials with *Fhb7^{The2}* or *Fhb1* alone.

Keywords: aneuploidy; bread wheat; disomic addition; ditelosomic addition; introgression; meiotic stability; Robertsonian translocation; Sequenom; SNP; *Thinopyrum*

Supported by the National Science Foundation of the United States of America, Grant IOS-2102953 to J.D. and H.-G.M. and by a Grant from U.S. Wheat and Barley Scab Initiative (USDA Agreement 58-2090-8-071) to J.D. and J.A.A.

https://doi.org/10.17221/104/2024-CJGPB

Fusarium head blight (FHB) is an important disease of wheat with serious epidemics in many parts of the world during the past one hundred years (Ma et al. 2020). The disease is primarily caused by the fungus *Fusarium graminearum* Swabe although other fungal species may be involved. An infection with the fungus produces shriveled grain, which reduces grain yield. Food produced from infected grain is harmful to human and animal health due to mycotoxins present in the grain.

Wheat FHB is best controlled by integrated management, which includes growing FHB-resistant cultivars (Alisaac & Mahlein 2023). FHB resistance has several components in wheat: resistance to initial infection (type I), resistance to spread of infection within the spike (type II), detoxification of mycotoxins, and others (for review see Ma et al. 2020). Several genes and numerous quantitative trait loci (QTLs) have been identified for each type of resistance in wheat (Ma et al. 2020). One of the most effective wheat genes for type II resistance is *Fhb1,* originally discovered in Chinese cultivar Sumai 3 (Waldron et al. 1999; Cuthbert et al. 2006). *Fhb1* has been widely deployed in improving FHB resistance, particularly in spring wheat breeding programs.

Important sources of FHB resistance in wheat are wild relatives of wheat (Jauhar & Peterson 1998). One of the best is genus *Lophopyrum* (Löve 1984), which are perennial caespitose grasses closely related to the rhizomatous wheatgrasses of genus *Thinopyrum* (Löve 1984), with which they are often combined taxonomically (Barkworth 1992). *Lophopyrum* species can be hybridized with wheat, and amphiploids have been developed from some of these hybrids. The most notable is the octoploid amphiploid AgCS, which was developed from hybridization of *T. aestivum* ($2n$ = $6x$ = 42, subgenomes AABBDD) cultivar (cv) Chinese Spring (CS) with an unknown accession of *L. elongatum* ($2n$ = $2x$ = 14, genomes EE) (Rommel & Jenkins 1959). Numerous cytogenetic stocks were developed from AgCS, including complete sets of disomic addition (DA) lines, ditelosomic addition (DTA) lines and disomic substitution (DS) lines (Dvorak 1980; Hart & Tuleen 1983; Dvorak & Chen 1984; Tuleen & Hart 1988). AgCS was also used to develop genome-wide introgression lines in wheat (Xu et al. 2020). A wealth of single chromosome introgression lines in wheat was developed from representative DS lines (Zhang et al. 2017, 2018, 2020, 2022).

Shen et al. (2004) screened the set of DS lines for FHB resistance and found high resistance levels in DS lines 7E(7A), 7E(7B) and 7E(7D). Follow-up studies confirmed these findings and located FHB resistance on chromosome arm 7EL (Miller et al. 2011; Fu et al. 2012). Due to the importance of *L. elongatum* as a source of FHB resistance, the genome of *L. elongatum* accession (acc.) PI 531718 was sequenced (Wang et al. 2020). Sequence analysis revealed that the *L. elongatum* genome present in AgCS was not equivalent to the genome of PI 531718 (Xu et al. 2020).

FHB resistance was also detected in DS line $7el_2$(7D) derived from *L. ponticum* (Zhang et al. 2011). The resistance gene was mapped on the long arm of $7el_2$ (Miller et al. 2011; Zhang et al. 2011; Guo et al. 2015) and introgressed into wheat (Forte et al. 2014; Guo et al. 2015). The gene was named *Fhb7* (Guo et al. 2015). FHB resistance was also introgressed into wheat from *L. elongatum* chromosome 7E, first via Robertsonian translocations with wheat chromosome 7D (Ceoloni et al. 2017; Haldar et al. 2021) and later by meiotic recombination with wheat chromosome 7B (Zhang et al. 2022).

Genetic mapping suggested that FHB resistance on 7E and $7el_2$ chromosomes was conferred by the same locus. The locus was identified in the *L. elongatum* acc. PI 531718 genome sequence as glutathione S-transferase (GST) (Wang et al. 2020). GST confers resistance in wheat by inactivating the deoxynivalenol (DON) mycotoxin (Hou et al. 2024). The gene is widely distributed in Triticeae (Guo et al. 2022). Zhang et al. (2022) designated the *L. ponticum* allele on $7el_2$ as $Fhb7^{Thp}$, that on 7E in PI 531718 as $Fhb7^{The1}$, and that on 7E in AgCS as $Fhb7^{The2}$. Alleles $Fhb7^{The1}$ and $Fhb7^{The2}$ differ from $Fhb7^{Thp}$ by five and seven missense mutations, respectively, whereas they differ from each other by two missense mutations (Zhang et al. 2022).

The *L. ponticum* $Fhb7^{Thp}$ allele was combined with *Fhb1* in wheat with the hope of generating FHB resistance higher than that conferred in wheat by either gene (Guo et al. 2015). Disappointingly, the level of FHB resistance did not differ from that of an *Fhb1* control (Guo et al. 2015). However, as the *L. ponticum* $Fhb7^{Thp}$ allele differs from the *L. elongatum* alleles $Fhb7^{The1}$ and $Fhb7^{The2}$, this outcome should not discourage further pursuit of the idea of combining these genes for achieving greater FHB resistance.

Here, we combined $Fhb7^{The2}$ with *Fhb1* and assessed FHB resistance in two different bread wheat genetic backgrounds. The source of $Fhb7^{The2}$ was introgression line IL45497 (Xu et al. 2020). The line was produced by recurrently self-pollinating a hybrid /AgCS × *ph1c*/× *ph1b,* where *ph1c* (Giorgi

https://doi.org/10.17221/104/2024-CJGPB

1978) and *ph1b* (Sears 1977) were deletion mutants of *Ph1* in durum wheat cv Cappelli and CS, respectively. IL45497 had 2*n* = 46 bibrachial chromosomes, which included recombined chromosome(s) with arms 2ES and 7EL and complete *L. elongatum* chromosome 5E. Two experimental lines were developed by recurrent backcrossing of IL45497 into spring wheat cv Rollag and MN-Washburn, both possessing *Fhb1*. They were characterized cytogenetically and genotyped with *L. elongatum* genome-specific Sequenom single nucleotide polymorphism (SNP) MassARRAY (Xu et al. 2020). FHB resistance of the two lines was compared with materials possessing single genes and negative controls.

MATERIAL AND METHODS

Plants. To combine $Fhb7^{The2}$ with *Fhb1*, IL45497 possessing $Fhb7^{The2}$ was crossed with spring bread wheat cv Rollag (Anderson et al. 2015) and MN-Washburn (Anderson et al. 2021), both possessing *Fhb1*. Hybrids were backcrossed twice to Rollag and MN-Washburn and self-pollinated for three and four generations, respectively. *Lophopyrum elongatum* DA line 7E in the CS genetic background (Dvorak 1980) was used as $Fhb7^{The2}$ control, and bread wheat cv Wheaton and CS were used as controls devoid of either gene.

Chromosome analyses. Introgression of $Fhb7^{The2}$ into the MN-Washburn and Rollag genetic backgrounds required routine determination of chromosome numbers and meiotic chromosome pairing. For root-tip chromosome analyses, seeds were germinated in Petri-dishes. Root-tips were excised and maintained in distilled water at 1 to 2 °C for 24 h. They were fixed in a 3 alcohol : 1 glacial acetic acid (v/v) fixative for 24 h, hydrolysed in 1N HCl at 60 °C for 10 min, stained in Schiff's reagent for 30 min and treated with a solution containing 0.2% pectinase (v/v) (SIGMA, CAS No. 9032-75-1) and 0.2% cellulase (w/v) (SIGMA, CAS No. 9012-54-8) for 20 min at room temperature. They were then stored at 5 °C in distilled water for 2 to 5 days before being used to reduce cell breakage during squashing (Dvorak 1971). Root-tip squashes were made in 1% acetocarmine. For meiotic analyses, immature spikes were fixed in 6 ethanol : 3 chloroform : 1 glacial acetic acid (v/v) for 24 h at room temperature. Spikes were then transferred into 70% ethanol for one day at room temperature. Meiocytes were then squashed in 1% acetocarmine for microscopic observations.

Genotyping. To design PCR primers for the detection of the GST gene on chromosome arm 7EL, the sequence of the gene transcript (Tel7E01T1020600.1) was downloaded from the *L. elongatum* acc. PI 531718 genome sequence assembly ASM1179987v1. Primers were designed with the Primer 3 program (Rozen & Skaletsky 2000). Since the *L. elongatum* genome present in AgCS differed from that of PI 531718 (Xu et al. 2020), the efficacy of each primer pair was tested by PCR using genomic DNAs of CS and DS lines 7E(7A), 7E(7B) and 7E(7D). Gene-specific amplification was obtained with forward primer AGACTGGCCCTCAACTTCAA and reverse primer AGTCTGCGAGCTCTGGTGAT. The pair was designated as UCD-Fhb7-3F3R.

DNA for PCR genotyping was isolated from leaves as described earlier (Dvorak et al. 2006). PCR was performed in 1× New England Biolabs (NEB) standard buffer, 0.2 mM each dNTP, 0.025 u/μL standard Taq DNA polymerase (NEB), 1 μM of each primer and 50 ng of genomic DNA. The cycling conditions were: 96 °C 5 min; 94 °C 30 s, 58 °C 30 s, 68 °C 3 min for 40 cycles; 68 °C 5 min; 10 °C hold. Amplicons were separated by 1.5% agarose gel electrophoresis.

The presence of *Fhb1* was detected with the KASP assay IFA-FM426_umn10 (Schweiger et al. 2016) and TaHRC-Kasp (Su et al. 2018). KASP assays were prepared with 12 μM of each allele-specific primer, and 24 μM of common reverse primer in molecular-grade water (Sigma Cat. No. 4502). Genotyping was performed in 8-μL reactions, consisting of 2 μL template DNA (normalized to 20 ng), 0.11 μL KASP assay, 4 μL 2X PACE™ master mix (3CR Bioscience, UK) and 1.89 μL molecular-grade water. KASP genotyping was conducted using the Roche Lightcycler® 480 with the following cycling conditions: an initial hot-start activation at 95° C for 15 min, followed by 10 touchdown cycles of 94 °C for 20 s and 61 °C for 1 min, with a decrement of –0.6 °C per cycle targeting a final temperature of 55 °C. This was followed by 38 additional cycles (for IFA-FM426_umn10) or 50 cycles (for TaHRC-KASP) at 94 °C for 20 s and 55 °C for 1 min. After a 2-min cool-down at 37 °C, an endpoint read was performed. Results were visualized on a 2D scatterplot, and alleles were called using the proprietary Lightcycler® 480 Endpoint Genotyping Software Module (Roche Diagnostics, Indianapolis, USA).

The presence and doses of *L. elongatum* chromosomes were confirmed by genotyping with the *L. elongatum* genome-specific Sequenom SNP MassARRAY

https://doi.org/10.17221/104/2024-CJGPB

(Xu et al. 2020). As a brief background about the markers, consider MassARRAY for chromosome 7. It consists of 19 multiplexed SNP markers. Marker AgCS7_339713115 exemplifies their naming and use in genotyping. The name indicates that it is an SNP between the wheat genome and the E genome in AgCS and it is located at 339 713 115 bp in the chr7 registry of *Ae. tauschii* genome assembly Aet v4.0 (Luo et al. 2017). The SNP consists of a T base on wheat chromosomes 7A, 7B, and 7D and an A base at an orthologous gene on *L. elongatum* chromosome 7E (Xu et al. 2020). The T is the low-mass base and A is the high-mass base at this Sequenom SNP assay. Detection of TA with the Sequenom assay indicates the presence of chromosome arm 7EL in a wheat genetic background whereas detection of T alone indicates its absence. Importantly, due to the unique properties of Sequenom SNP detection, most of the assays were sensitive enough to discriminate between the monosomic and disomic doses of added *L. elongatum* chromosomes in the wheat genetic background. The genotyping results were visualized in a 2D plot of base masses. The plots were used to determine the doses of *L. elongatum* chromosomes.

The presence of arm 2ES was detected with the dominant suppressor of waxy bloom on stems (Dvorak 1980). The presence of chromosome 5E was not monitored.

FHB reaction evaluation at Ottawa Research and Development Center, Agriculture and Agri-Food Canada, Ottawa, Canada in the Spring of 2018. The plants were grown in a Conviron walk-in growth room with temperature for the inoculation period maintained at 25 °C and 16-h photoperiod provided by light energy of 1 000 mEm^{-2} s^{-1}. Ten µL of inoculum of 50 000 conidia/mL consisting of three aggressive strains of *F. graminearum* were applied to a single floret in a spike at anthesis. Two to three spikes per plant were inoculated. Plants with inoculated spikes were placed in the mist bed of the growth chamber for 48 h with 80–90% humidity by 30 s pulses of mist released every hour. The plants were then moved to another bench in the growth chamber with 80% humidity and 25 °C. The number of infected spikelets on each inoculated spike was recorded 21 days after inoculation.

FHB reaction evaluation at the Department of Agronomy and Plant Genetics, University of Minnesota, St. Paul, USA in the Spring and Fall of 2022. Plant reactions to inoculation with conidia of *F. graminearum* in the greenhouse were evaluated using a technique described earlier (Anderson et al. 2001). The greenhouse trial was duplicated in the Spring and Fall of 2022. Briefly, spikes of the same size and maturity were inoculated at anthesis with a 10-µL droplet (100 000 conidia/mL) of conidial suspension placed directly into a single spikelet near the center of the spike. The inoculum was from the Butte86ADA-11 isolate, and almost certainly differed from the inoculum used at the Ottawa Research and Development Center. An inoculated spike was covered with a plastic bag. In the Spring of 2022, the bags were removed from the spikes after 3 days. In the Fall of 2022, each family was divided into two approximately equal groups and plastic bags were removed after 3 or 4 days, to assess the effects of the length of spike covering on the infection rate. The percentage of infected spikelets out of the total spikelet number on a spike was visually scored.

Statistical analysis of FHB reaction data. The density of spikelet infection rates produced at the Department of Agronomy and Plant Genetics, University of Minnesota were not normally distributed. The distribution showed sharp peaks at several levels, indicating the existence of point masses in the original data, and this issue could not be resolved through transformation. These point masses may have been due to the unequal sizes of the samples, which ranged from 15 to 49 plants. Even the most effective transformation among those considered, namely the arccosine square root transform, resulted in a distribution with heavy tail and point masses.

To address this issue, we discretized the response variable into three groups: low-, medium-, and high-infection levels, with cutoff points of 0.09 and 0.14, which ensured that the group sizes of the three levels were balanced. After this discretization step, we employed two proportional odds models to investigate the relationships between the explanatory variables and the ordinal response variable. The proportional odds model is a parsimonious extension of the logistic regression model for multi-category ordinal responses (McCullagh 2019).

The proportional odds analysis involved the fitting of two models, aiming to evaluate the impact of the *Fhb1* and $Fhb7^{The2}$ genes on infection rates and to evaluate differences between genetic backgrounds. The first proportional odds model can be written as

$$\text{logit}\,(\Pr(\text{low infection level})) = \beta_{01} + \beta_1 1_{Gene=Fhb7^{The2}} + \\ + \beta_2 1_{Gene=Fhb1,Fhb7^{The2}} + \beta_3 1_{Line=Rollag-DA},$$

https://doi.org/10.17221/104/2024-CJGPB

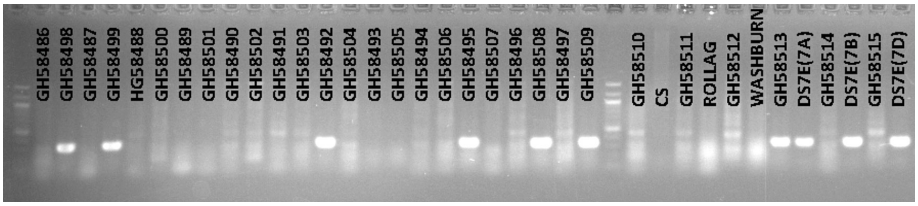

Figure 1. Amplification of *Fhb7*^{The2} with the UCD-Fhb7-3F3R PCR primers; the primer pair amplified a 333-bp product in DNA of DS lines 7E(7A), 7E(7B), and 7E(7D) but no meaningful product was observed in DNA of CS, MN-Washburn, and Rollag; a product of the same size was amplified in 7 of 31 plants of BC_2F_2 MN-Washburn backcross progeny of plant GH58138 (for pedigree see Figure 2A); a NEB 100-bp size ladder with smallest prominent band 500 bp long is in lanes 1 and 26

$$\text{logit}\,(\Pr(\text{low infection level and medium infection level})) = \beta_{02} + \beta_1 1_{Gene=Fhb7T^{he2}} + \\ + \beta_2 1_{Gene=Fhb1,Fhb7^{The2}} + \beta_3 1_{Line=Rollag-DA},$$

where the link function is defined as

$$\text{logit}(p) = \log\left(\frac{p}{1-p}\right)$$

with the constraint that $\beta_{01} \leq \beta_{02}$. The first slope coefficient β_1 quantified the distinction of the effects of *Fhb1* and *Fhb7*^{The2} and the second slope coefficient β_2 the distinction of the effects between *Fhb1* and *Fhb1* + *Fhb7*^{The2}. The third slope coefficient β_3 allowed the identification of the difference of the effects between genetic backgrounds harboring *Fhb1* and *Fhb7*^{The2}. Note that the difference between the effects of *Fhb7*^{The2} and *Fhb1*+*Fhb7*^{The2} can be determined by $\beta_2 - \beta_1$. The maximum likelihood estimators of the model coefficients were obtained with the function "polr" in the R package.

To compare the differences in infection levels among the cultivars MN-Washburn, CS, and Rollag, the following second proportional odds model was utilized,

$$\text{logit}\,(\Pr(\text{low infection level})) = \alpha_{01} + \\ \alpha_1 1_{Gene=Fhb1,Fhb7^{The2}} + \alpha_2 1_{Variety=Rollag} + \\ + \alpha_3 1_{Variety=MN-Washburn},$$

$$\text{logit}\,(\Pr(\text{low infection level and medium infection level})) = \alpha_{02} + \alpha_1 1_{Gene=Fhb1,Fhb7^{The2}} + \\ + \alpha_2 1_{Variety=Rollag} + \alpha_3 1_{Variety=MN-Washburn},$$

with the constraint $\alpha_{01} \leq \alpha_{02}$. The coefficient α_1 identifies the effect of combined genes *Fhb1*+*Fhb7*^{The2}. The coefficients α_2, α_3, and $\alpha_3 - \alpha_2$ differentiate among the cultivars Rollag, MN-Washburn, and CS.

RESULTS

***Fhb7*^{The2}-specific primer development.** PCR primer pair UCD-Fhb7-3F3R amplified a single 333 bp-product in DNA of DS lines 7E(7A), 7E(7B) and 7E(7D), while no meaningful product was observed in DNA of CS, MN-Washburn, or Rollag (Figure 1). The detection of the *Fhb7*^{The2} gene is illustrated with genomic DNA of 29 BC_2F_2 plants of IL45497 × MN-Washburn backcrossed to MN-Washburn. The 333 bp product was present in DNA of 6 plants and absent from DNA of the reminding 24 plants (Figure 1). All 7 positive plants had a telosome added to 42 wheat chromosomes in the root-tips, while no telosome was observed in the root-tips of the remaining 24 plants. The agreement between genotyping and cytological results confirmed that PCR specifically detected the 7EL chromosome arm.

Combining *Fhb7*^{The2} with *Fhb1*. In a preliminary step, reactions to FHB inoculation was investigated in two families of introgression line IL45497 and compared to reactions of CS and *ph1c* line, the parents of IL45497. Both IL45497 families showed elevated FHB resistance compared to those in CS and *ph1c* (Table 1). As all CS and *ph1c* plants showed 100%

Table 1. Infection rates expressed as percent of infected spikelets in two families of IL45497 bearing *Fhb7*^{The2} and parental cultivar Chinese Spring and *ph1c* mutant line without the gene in June, 2018 at Agriculture Canada Station, Ottawa, Canada

Cultivar or line	Family	*Fhb7*^{The2}	Plants (No.)	Infected spikelets (%)
Chinese Spring		no	10	100
ph1c line		no	13	100
IL45497	No. 1	yes	16	34
IL45497	No. 2	yes	23	24

https://doi.org/10.17221/104/2024-CJGPB

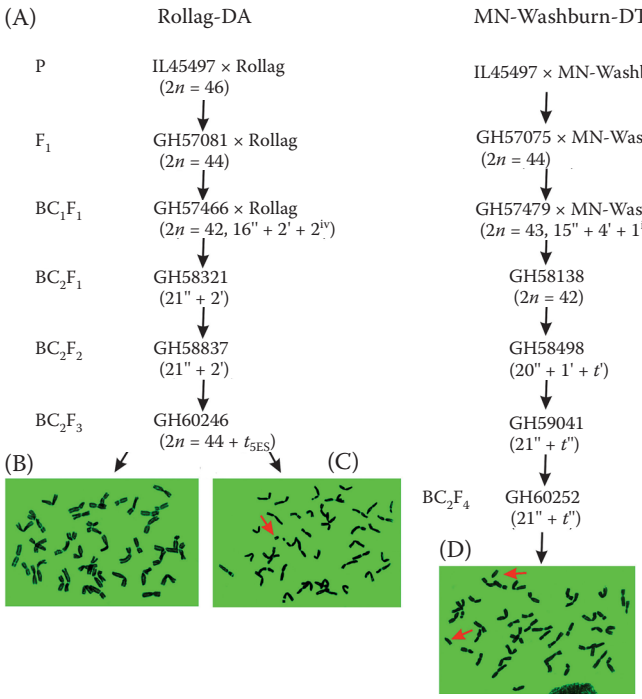

Figure 2. Development and characterization of Rollag-DA and MN-Washburn-DTA lines: (A) pedigrees leading to the development of Rollag-DA (plant GH60246) and MN-Washburn-DTA (plant GH59041); chromosome numbers and meiotic pairing of the plants are indicated in parentheses; the root-tip counts are preceded by 2*n;* Meiotic chromosome pairing is also shown if it was determined; the univalent, bivalent, trivalent, quadrivalent and quinquevalent MI configurations are indicated by ', '', '''', ^{iv}, and ^{v}, respectively; (B) a root-tip metaphase plate with 2*n* = 44 in a GH60246 progeny plant; (C) a root-tip metaphase plate with 2*n* = 44 + *t* (arrow) in a GH60246 progeny plant; (D) a root-tip metaphase plate with 2*n* = 42 + 2 *t* (arrows) in a GH60252 progeny plant

infection rate with zero variance, these results were not subjected to statistical treatment. Nevertheless, the great difference between the responses of CS and *ph1c* line on one hand and IL45497 on the other hand was consistent with 7EL in IL45497 possessing *Fhb7*^{The2}.

IL45497 was crossed with the *Fhb1*-bearing cultivars Rollag and MN-Washburn. Both F_1 progeny had 44 chromosomes in root-tips, as expected from 2*n* = 46 in IL45497, and were backcrossed to the respective wheat parent (Figure 2A). The BC_1F_1 plants GH57466 and GH57479 derived from the backcrosses had complex chromosome pairing at metaphase I (MI) (Figure 2A). The second backcross to Rollag and MN-Washburn was then made (Figure 2A).

In the second backcross to Rollag, 2ES and 7EL arms were usually transmitted together to progeny. For example, of 27 BC_2F_2 plants positive for the UCD-Fhb7-3F3R marker, 23 plants were devoid of wax on stems, indicating that they also received arm 2ES. Four plants that had a waxy bloom on stems, indicating the absence of 2ES, had either a telosome or isosome at MI in meiosis. Plant GH60246 (Figure 2A) that was positive for the UCD-Fhb7-3F3R marker and had 22 bivalents plus a short telosome was obtained in the BC_2F_3 generation. Root-tip chromosomes were analysed in seven progeny of this plant. Six of them had 2*n* = 44 chromosomes (Table 2, Figure 2B) and one had a short telosome in addition to the 44 bibrachial chromosomes (Table 2, Figure 2C). The seven plants were genotyped with the *L. elongatum* Sequenom SNP MassARRAY. All had both 2ES and 7EL chromosome arms (Figure 3A). Plant GH67013, which had 2*n*=44 + *t,* had a 5ES chromosome arm in addition to arms 2ES and 7EL (Figure 3A). These data were consistent and showed that the two *L. elongatum* arms formed a single 2ES·7EL chromosome, which was retrospectively already present in IL45497. A pair of this 2ES·7EL chromosome was added here to the wheat genome. This DA line was therefore named as Rollag-DA.

Table 2. Chromosome numbers in two families of MN-Washburn-DTA and one family of Rollag-DA

Line	Generation	Progeny	Plants (No.)	2*n*					
				42 + 2 *t*	42 + *t*	43 + 2 *t*	41 + 2 *t*	44	44 + *t*
MN-Washburn-DTA	BC_2F_5	GH60251	19	16 (84.2)	1 (5.2)	1 (5.2)	1 (5.2)		
MN-Washburn-DTA	BC_2F_5	GH60252	20	19 (95.0)		1 (5.0)			
Rollag-DA	BC_2F_4	GH60246	7					6 (85.7)	1 (14.3)

Percentages are in parentheses

https://doi.org/10.17221/104/2024-CJGPB

In the second backcross to MN-Washburn, BC_2F_2 plant GH58498 had a telosome substituted for an unknown wheat chromosome (Figure 2A). The plant was positive for the UCD-Fhb7-3F3R marker, but had waxy bloom on stems, indicating the absence of chromosome arm 2ES. Plant GH59041 positive for the UCD-Fhb7-3F3R marker and having 42 chromosomes plus a pair of homologous telosomes (Figures 2A, D) was encountered among BC_2F_3 progeny. The plant was selfed, and its BC_2F_5 progeny was genotyped with the Sequenom SNP MassARRAY. All progeny plants had chromosome arm 7EL, but not arms 2ES or 5ES (Figure 3A). These data were consistent and showed that this backcross resulted in the ditelosomic addition of 7EL arm to the wheat genome. This line was therefore named as MN-Washburn-DTA.

The results of Sequenom assays for each of the 14 SNP markers on 7EL in five Rollag BC_2F_4 plants and seven MN-Washburn BC_2F_5 plants, along with those for three plants of monosomic addition (MA) 7E, a single plant of DS line 7E(7D), and a single plant of CS were plotted (Figure 3B). Sequenom base mass yields for all BC_2F_4 and BC_2F_5 plants clustered together. Their cluster was between the cluster for three MA 7E plants and the single plant of DS line 2E(2D) (Figure 3B). These cluster positions were consistent with the ratios of wheat to *L. elongatum* bases expected in the following genotypes: 2 : 1 in the DS, 3 : 1 in DA, and 6 : 1 in MA. Clustering of base mass yields in the plots was consistent with chromosome analysis and provided additional evidence that the Rollag backcross resulted in adding a pair of 2ES·7EL

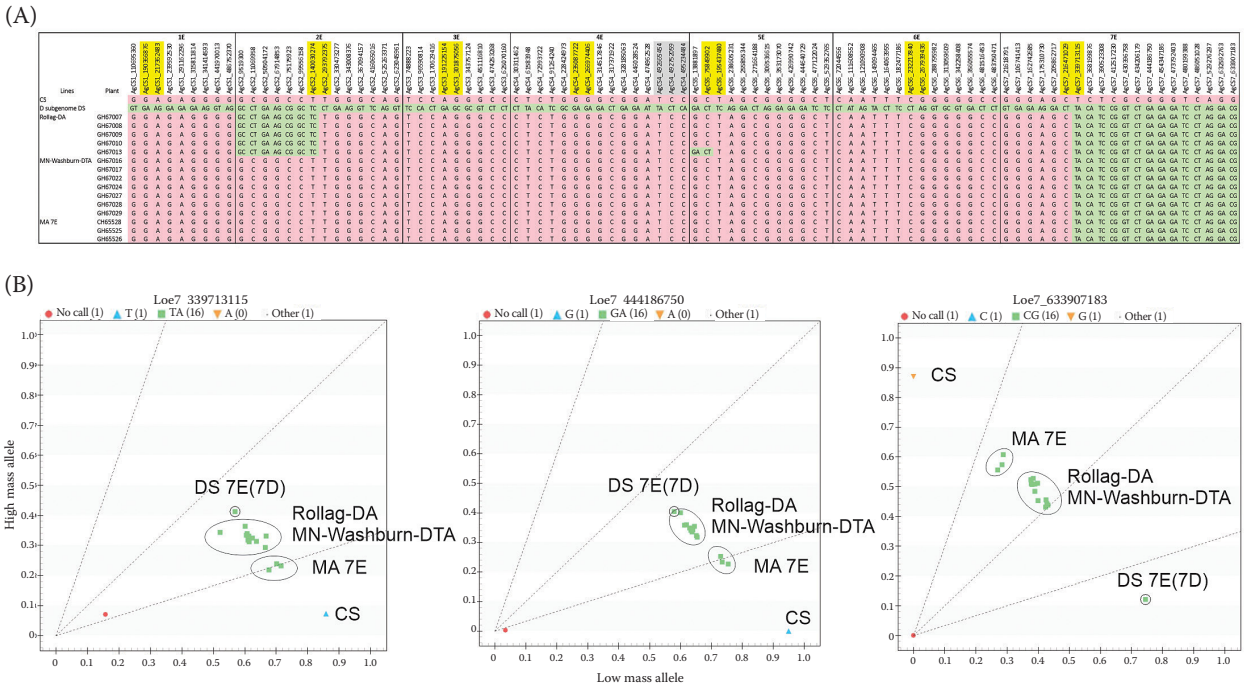

Figure 3. Sequenom SNP genotyping; genotype positions in a plot reflect the ratio of the low-mass allele yield and high-mass allele yield; the dotted lines delimit the yields; if two alleles are 1 : 1, as in a heterozygous diploid, the ratio is expected to be near the diagonal line. If the high-mass and low-mass alleles are in a 2:1, 3:1 or even more extreme ratio, the mass yield is expected to be in a sector either above or below the diagonal; (A) genome-wide sequenom genotyping with sequenom SNP markers of five GH60246 progeny plants (Rollag-DA) and seven GH60252 progeny plants (MN-Washburn-DTA), the seven possible D-subgenome DS lines and CS; numbers in the marker names are locations in the bp registry of *Ae. tauschii* genome sequence Aet v4.0 (Luo et al. 2017); the centromere is between markers in yellow cells; if a marker genotype indicated the presence of the *L. elongatum* base, the cell is green; if it indicated the absence of the *L. elongatum* base, the cell is red; (B) plots of low- and high-mass base yields for three SNP markers on 7EL; plotted are mass yields for five plants of Rollag-DA, seven plants of MN-Washburn-DTA, three MA 7E plants, one plant of DS line 7E(7D), and one plant of CS; from the left: the most proximal 7EL SNP marker (AgCS7_339713115), a middle of the arm marker (AgCS7_444186750), and the most distal 7EL SNP marker (AgCS7_633907183); the cluster of mass yields for Rollag-DA and MN-Washburn-DTA plants (3 : 1 allele ratio) is always between the cluster of three MA 7E plants (6 : 1 allele ratio) and that of one plant of DS 7E(7D) (2 : 1 allele ratio)

https://doi.org/10.17221/104/2024-CJGPB

chromosomes to the wheat genome whereas the MN-Washburn backcross resulted in adding a pair of 7EL telosomes to the wheat genome.

The DA and DTA states were stable. Of 39 BC_2F_5 MN-Washburn-DTA plants in two families derived from plant GH59041 (Figure 2A), only one plant was not a DTA (Table 2). Three plants were aneuploid for wheat chromosomes. The DA state in progeny of plant GH60246 (Table 2) was also stable, although only seven plants were investigated (Table 2).

To assess the status of *Fhb1* in these families, 10 progeny plants of Rollag-derived BC_2F_2 plant GH58837, which was the parent of plant GH60246 (Figure 2A), and was heterozygous for the UCD-Fhb7-3F3R marker were genotyped with the IFA-FM426-umn10 (Schweiger et al. 2016) and TaHRC (Su et al. 2018) markers diagnostic for *Fhb1*. All 10 plants were positive for the *Fhb1* markers suggesting that GH58837 was likely homozygous for *Fhb1* ($P = 0.068$, χ^2 with 1 df). Likewise, 14 progeny plants of MN-Washburn-derived BC_2F_2 plant GH58498, the parent of plant GH59041 (Figure 2A), were positive for the *Fhb1* markers suggesting that GH5498 was homozygous for *Fhb1* ($P = 0.031$, χ^2 with 1 df). Thus, *Fhb1* and *Fhb7*^{The2} were combined in MN-Washburn-DTA and Rollag-DA and both lines were homozygous for the two genes.

FHB infection rates. MN-Washburn-DTA and Rollag-DA, which possessed both genes, MN-Washburn and Rollag which possessed *Fhb1* only, DA 7E which possessed *Fhb7*^{The2} only, and Wheaton and CS, which possessed neither of the genes, were inoculated with *Fusarium* in a replicated greenhouse trial in the Spring and Fall of 2022 (Table 3). In the Spring of 2022, spikes were covered with plastic bags for 3 days after inoculation. In the Fall of 2022, each progeny was divided into two approximately equal groups and spikes were covered for three and four days after inoculation, to find if the length of covering a spike with a plastic bag affected the infection rate. Except for MN-Washburn, the days for which spikes were covered with bags had no significant effect on mean spike infection rates (*t*-tests with Bonferroni correction in Table S1 in Electronic Supplementary Material (ESM)). For an unknown reason, MN-Washburn spikes covered for 3 days showed significantly lower spikelet infection rates than the cohort covered for 4 days ($P = 0.003$, *t*-test with Bonferroni correction) (Table S1 in ESM). Overall, the densities of infection rates (Figure 4A) and variances (Table S1 in ESM) were similar ($P = 0.79$, paired *t*-test) for the two treatments. The test thus validated covering of spikes with plastic bags for 3 days, as it was done in the Spring of 2022.

As pointed out in Methods and is apparent in Figures 4A and 4B, most of the spikelet infection rate data did not follow normal distribution. As transformation by arccosine square root did not resolve the distribution of response variables, the response variables (Table S1 in ESM) were discretized by group-

Table 3. Infection rates expressed as percent of infected spikelets in wheat cultivars or experimental lines with *Fhb1*, *Fhb7*^{The2}, combined *Fhb1* plus *Fhb7*^{The2}, or neither gene in trials conducted in the Spring and Fall of 2022 at the Department of Agronomy and Plant Genetics, University of Minnesota, St. Paul

Cultivar or line	Family	Genes	Spring 2022		Fall 2022	
			plants (No.)	infected spikelets (%)	plants (No.)	infected spikelets (%)
Wheaton		neither	34	93.9[a]	44	97.0[a]
CS		neither	18	63.9[b]		
DA 7E		*Fhb7*^{The2}	15	29.4[c]		
MN-Washburn		*Fhb1*	43	36.2[c]	33	23.0[c]
Rollag		*Fhb1*	39	29.0[c]	37	27.2[c]
MN-Washburn-DTA	GH59041	*Fhb1* + *Fhb7*^{The2}	35	8.2[d]	42	12.8[d]
MN-Washburn-DTA	GH60252	*Fhb1* + *Fhb7*^{The2}	42	9.1[d]	46	10.9[d]
MN-Washburn-DTA	GH60254	*Fhb1* + *Fhb7*^{The2}			35	10.1[d]
MN-Washburn-DTA	GH60255	*Fhb1* + *Fhb7*^{The2}	43	8.8[d]	40	10.9[d]
Rollag-DA	GH60246	*Fhb1* + *Fhb7*^{The2}	40	9.4[d]	49	12.2[d]

Means followed by a common letter are not significantly different at $P = 0.001$ level (based on pairwise comparisons of proportional odds model)

https://doi.org/10.17221/104/2024-CJGPB

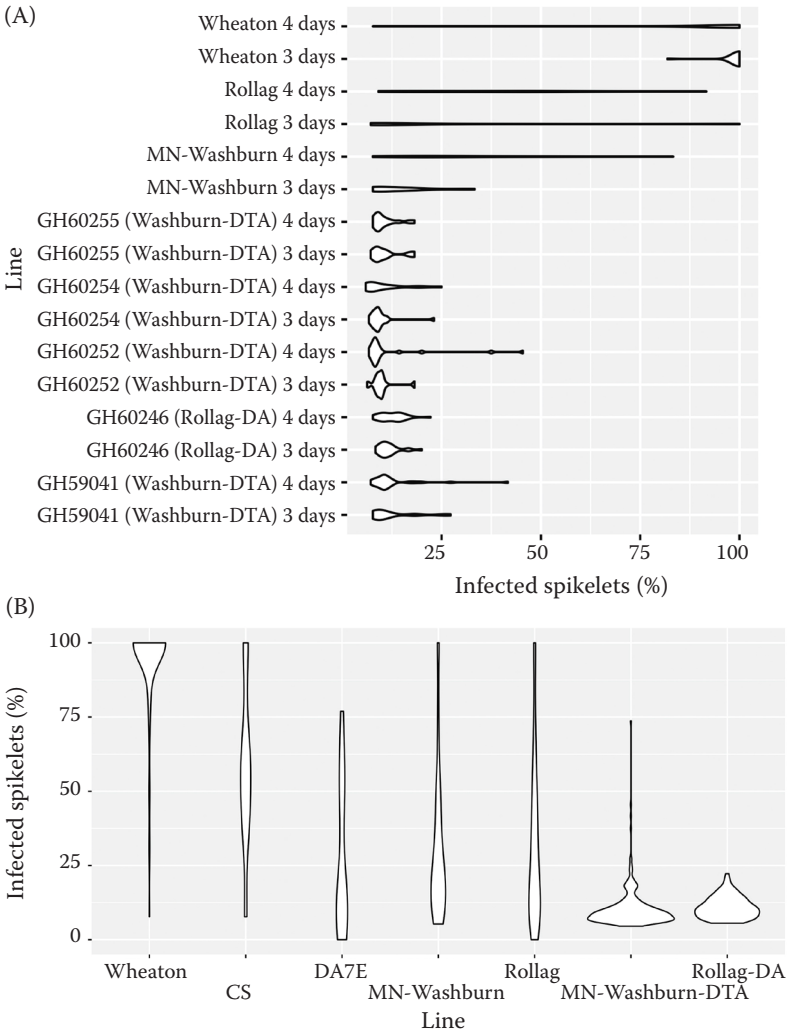

Figure 4. Violin plots of densities of FHB spikelet infection rates: (A) densities of spikelet infection rates in spikes covered with plastic bags for 3 or 4 days after inoculation in families with both genes (Rollag-DA and MN-Washburn-DTA), with *Fhb1* only (Rollag and MN-Washburn), and neither gene (CS and Wheaton) in the Fall of 2022; (B) densities of combined spikelet infection rates in the Spring and Fall of 2022.

ing them into three groups: low-, medium-, and high-infection levels, with cutoff points of 0.09 and 0.14, which ensured that the group sizes of the three levels were balanced. The maximum likelihood estimates of the coefficients of the proportional odds models along with their corresponding *P*-values were computed (Table 4). A significant negative β_2 coefficient estimate indicated that Rollag-DA and MN-Washburn-DTA jointly had significantly lower infection rates than the parental cv Rollag and MN-Washburn possessing *Fhb1* and DA 7E possessing *Fhb7*^{The2} (P < 1e-3). A non-significant estimated β_1 coefficient (P = 0.2) suggested that in this study the resistance levels to FHB provided by *Fhb1* (in Rollag and MN-Washburn) could not be distinguished from those provided by *Fhb7*^{The2} (in DA 7E).

In the second model, a significantly negative coefficient α_1 identifying the effect of combined genes *Fhb1* and *Fhb7*^{The2} compared to either *Fhb1* present in Rollag and MN-Washburn or *Fhb7*^{The2} present in DA 7E was significant (P < 1e-3), but coefficients α_2, α_3, and $\alpha_3 - \alpha_2$ discriminating among Rollag, MN-Washburn, and CS were not significant (Table 5).

Table 4. Coefficients (maximum likelihood estimates) and *P*-values for the first proportional odds model

Coefficient	Estimate	*P*-value
β_1	–0.69	0.20
β_2	–2.17	$< 10^{-9}$
$\beta_2 - \beta_1$	–1.49	0.004
β_3	0.67	0.002

Table 5. Coefficients (maximum likelihood estimates) and their *P*-values for the second proportional odds model

Coefficient	Estimate	*P*-value
α_1	–1.91	$< 10^{-9}$
α_2	0.83	0.13
α_3	0.52	0.33
$\alpha_3 - \alpha_2$	–0.31	0.10

https://doi.org/10.17221/104/2024-CJGPB

DISCUSSION

Fhb1 and *Fhb7* individually provide improved levels of FHB resistance in wheat. To find if combining these genes would have synergistic effects and confer even higher levels of resistance in wheat, introgression line IL45497 with 2*n* = 46 and possessing *L. elongatum* chromosome 5E and chromosome arms 2ES and 7EL (Xu et al. 2020) was recurrently backcrossed to *Fhb1*-bearing bread wheat cultivars Rollag and MN-Washburn. The backcross to Rollag resulted in adding to the wheat genome a pair of 2ES·7EL chromosomes, which most likely originated by Robertsonian translocation between *L. elongatum* chromosomes 2E and 7E during the development of IL45497. This DA line was designated as Rollag-DA. The backcross to MN-Washburn resulted in adding a pair of 7EL telosomes to the wheat genome, and the line was designated as MN-Washburn-DTA.

Of 39 plants of MN-Washburn-DTA, only one plant was not ditelosomic. A similar stability of the added chromosome pair was observed in Rollag-DA. As both lines were homozygous for $Fhb7^{The2}$ and *Fhb1* and transmitted the genes normally to progeny, they were an adequate experimental material for evaluating the combined effects of the two genes on FHB infection rates.

The FHB resistance was evaluated in the controlled environment of a greenhouse rather than a field environment. The evaluation of resistance required quantifying infection rates in plants differing in heading dates. Quantitative comparisons of such material would be difficult in the field, where temperature and humidity vary from day to day. In the greenhouse, all plants were inoculated at anthesis, which is when wheat is most receptive to inoculation, and inoculation was conducted over several dates to maximize its uniformity across the lines. The temperature and humidity could be constant during and after inoculations. For the deployment of the results in wheat breeding, it is nevertheless important to verify the greenhouse results under field conditions.

Based on the greenhouse trials, combining $Fhb7^{The2}$ with *Fhb1* conferred higher levels of type II FHB resistance in wheat than *Fhb1* or $Fhb7^{The2}$ alone. This result differed from a previous investigation of synergy of *Fhb1* and *Fhb7,* in which the *L. ponticum* $Fhb7^{Thp}$ allele was combined with *Fhb1* (Guo et al. 2015). In that study, combining the two genes failed to produce higher levels of resistance than expressed in Ning 7840 bearing *Fhb1* or introgression lines SDAU1881 and SDAU1886 bearing $Fhb7^{Thp}$. As the $Fhb7^{Thp}$ and $Fhb7^{The2}$ alleles differ by seven missense mutations (Zhang et al. 2022), it is possible that different outcomes in these two studies were due to genetic differences between $Fhb7^{Thp}$ and $Fhb7^{The2}$ rather than confounding effects of genetic background. It is, for instance, unlikely that the presence of 2ES and occasional presence of 5ES in Rollag-DA caused the difference, since neither chromosome 2E nor chromosome 5E conferred resistance in DS lines (Shen et al. 2004; Miller et al. 2011; Fu et al. 2012). In addition, 2ES and 5ES were absent from the MN-Washburn-DTA line, yet the line did not show diminished FHB resistance. It is also unlikely that the difference was due to residual genes from the CS or *ph1c* genetic backgrounds that could have been present in Rollag-DA and MN-Washburn-DTA lines. Although CS is known to have some resistance to FHB (Grausgruber et al. 1999; Ma et al. 2006), the CS genetic background was diluted during the development of IL45497 and its backcrossing into MN-Washburn or Rollag.

Synergy of *Fhb1* with $Fhb7^{The2}$ observed here is consistent with resistance obtained with transgenic strains of the endophytic fungus *Phomopsis liquidambaris.* The presence of both *Fhb1* and *Fhb7* genes in engineered strains had synergistic effects on FHB resistance in wheat (Wang et al. 2023).

It must be emphasized that the goal of this study was to assess the effects of combining $Fhb7^{The2}$ with *Fhb1* on FHB infection rates, not to develop material for wheat breeding. In both lines with $Fhb7^{The2}$ and *Fhb1*, the former gene was on an added chromosome, either 2ES·7EL or telosome 7EL. Although the DA and DTA states were stable and normally transmitted $Fhb7^{The2}$ to self-pollinated progeny, the added chromosomes and with them $Fhb7^{The2}$ would almost certainly be lost if included into a breeding program without extensive cytogenetic monitoring. Fortunately, an excellent introgression material exists with $Fhb7^{The2}$ on a short terminal 7EL segment recombined with wheat chromosome 7B (Cai et al. 2024). As such a chromosome is expected to pair in meiosis with a wheat homologue, it can readily be used in wheat breeding programs and serve as a vehicle for combining $Fhb7^{The2}$ with *Fhb1* with the goal of developing highly FHB resistant wheat varieties.

REFERENCES

Alisaac E., Mahlein A.K. (2023): Fusarium head blight on wheat: Biology, modern detection and diagnosis and integrated disease management. Toxins, 15: 192.

https://doi.org/10.17221/104/2024-CJGPB

Anderson J.A., Stack R.W., Liu S., Waldron B.L., Fjeld A.D., Coyne C., Moreno-Sevilla B., Fetch J.M., Song Q.J., Cregan P.B., Frohberg R.C. (2001): DNA markers for Fusarium head blight resistance QTLs in two wheat populations. Theoretical and Applied Genetics, 102: 1164–1168.

Anderson J.A., Wiersma J.J., Linkert G.L., Reynolds S., Kolmer J.A., Jin Y., Dill-Macky R., Hareland G.A. (2015): Registration of 'Rollag' Spring Wheat. Journal of Plant Registrations, 9: 201–207.

Anderson J.A., Wiersma J.J., Reynolds S.K., Conley E.J., Caspers R., Linkert G.L., Kolmer J.A., Jin Y., Rouse M.N., Dill-Macky R., Smithy M.J., Dykes L., Ohm J.B. (2021): Registration of 'MN-Washburn' hard red spring wheat containing resistance gene. Journal of Plant Registrations, 15: 490–503.

Barkworth M.E. (1992): Taxonomy of the Triticeae: A historical perspective. Hereditas, 116: 1–14.

Cai X.W., Danilova T., Charif A., Wang F., Zhang W., Zhang M.Y., Ren S.F., Zhu X.W., Zhong S.B., Dykes L., Fiedler J., Xu S., Frels K., Wegulo S., Boehm J., Funnell-Harris D. (2024): Registration of WGC002 spring wheat containing wild grass-derived Fusarium head blight resistance gene. Journal of Plant Registrations, 18: 179–186.

Ceoloni C., Forte P., Kuzmanovic L., Tundo S., Moscetti I., De Vita P., Virili M.E., D'Ovidio R. (2017): Cytogenetic mapping of a major locus for resistance to Fusarium head blight and crown rot of wheat on *Thinopyrum elongatum* 7EL and its pyramiding with valuable genes from a *Th. ponticum* homoeologous arm onto bread wheat 7DL. Theoretical and Applied Genetics, 130: 2005–2024.

Cuthbert P.A., Somers D.J., Thomas J., Cloutier S., Brule-Babel A. (2006): Fine mapping *Fhb1*, a major gene controlling fusarium head blight resistance in bread wheat (*Triticum aestivum* L.). Theoretical and Applied Genetics, 112: 1465–1472.

Dvorak J. (1971): Reducing breakage of metaphase plates in Feulgen stained root tips of wheat; ice water storage before squashing. Stain Technology, 46: 93–94.

Dvorak J. (1980): Homoeology between *Agropyron elongatum* chromosomes and *Triticum aestivum* chromosomes. Canadian Journal of Genetics and Cytology, 22: 237–259.

Dvorak J., Chen K.C. (1984): Phylogenetic relationships between chromosomes of wheat and chromosome 2E of *Elytrigia elongata*. Canadian Journal of Genetics and Cytology, 26: 128–132.

Dvorak J., Akhunov E.D., Akhunov A.R., Deal K.R., Luo M.C. (2006): Molecular characterization of a diagnostic DNA marker for domesticated tetraploid wheat provides evidence for gene flow from wild tetraploid wheat to hexaploid wheat. Molecular Biology and Evolution, 23: 1386–1396.

Forte P., Virili M.E., Kuzmanovic L., Moscetti I., Gennaro A., D'Ovidio R., Ceoloni C. (2014): A novel assembly of *Thinopyrum ponticum* genes into the durum wheat genome: pyramiding Fusarium head blight resistance onto recombinant lines previously engineered for other beneficial traits from the same alien species. Molecular Breeding, 34: 1701–1716.

Fu S.L., Lv Z.L., Qi B., Guo X., Li J., Liu B., Han F.P. (2012): Molecular cytogenetic characterization of wheat-*Thinopyrum elongatum* addition, substitution and translocation lines with a novel source of resistance to wheat Fusarium head blight. Journal of Genetics and Genomics, 39: 103–110.

Giorgi B. (1978): A homoeologous pairing mutant isolated in *Triticum durum* cv. Cappelli. Mutation Breeding Newsletter, 11: 4–5.

Grausgruber H., Lemmens M., Bürstmayr H., Ruckenbauer P. (1999): Resistance of 'Chinese Spring' substitution lines carrying chromosomes from 'Cheyenne', 'Hope' and 'Lutescens 62' wheats to head blight caused by *Fusarium culmorum*. Hereditas, 130: 57–63.

Guo J., Zhang X.L., Hou Y.L., Cai J.J., Shen X.R., Zhou T.T., Xu H.H., Ohm H.W., Wang H.W., Li A.F., Han F.P., Wang H.G., Kong L.R. (2015): High-density mapping of the major FHB resistance gene *Fhb7* derived from *Thinopyrum ponticum* and its pyramiding with *Fhb1* by marker-assisted selection. Theoretical and Applied Genetics, 128: 2301–2316.

Guo X.R., Wang M., Kang H.Y., Zhou Y.H., Han F.P. (2022): Distribution, polymorphism and function characteristics of the GST-encoding *Fhb7* in Triticeae. Plants-Basel, 11: 2074.

Haldar A., Tekieh F., Balcerzak M., Wolfe D., Lim D., Joustra K., Konkin D., Han F.P., Fedak G., Ouellet T. (2021): Introgression of *Thinopyrum elongatum* DNA fragments carrying resistance to fusarium head blight into *Triticum aestivum* cultivar Chinese Spring is associated with alteration of gene expression. Genome, 64: 1009–1020.

Hart G.E., Tuleen N.A. (1983): Chromosomal control of eleven *Elytrigia elongata* (=*Agropyron elongatum*) isozyme structural genes. Genetic Research, 41: 181–202.

Hou B.Q., Wang D.W., Yan F.F., Cheng X.X., Xu Y.C., Xi X.P., Ge W.Y., Sun S.L., Su P.S., Zhao L.F., Lyu Z., Hao Y.C., Wang H.W., Kong L.R. (2024): Fhb7-GST catalyzed glutathionylation effectively detoxifies the trichothecene family. Food Chemistry, 439: 138057.

Jauhar P.P., Peterson T.S. (1998): Wild relatives of wheat as sources of Fusarium head blight. National FHB Forum: 77–79.

Löve A. (1984): Conspectus of the Triticeae. Feddes Repertorium, 95: 425–521.

Luo M.C., Gu Y.Q., Puiu D., Wang H., Twardziok S.O., Deal K.R., Huo N.X., Zhu T.T., Wang L., Wang Y., McGuire

https://doi.org/10.17221/104/2024-CJGPB

P.E., Liu S.Y., Long H., Ramasamy R.K., Rodriguez J.C., Van S.L., Yuan L.X., Wang Z.Z., Xia Z.Q., Xiao L.C., Anderson O.D., Ouyang S.H., Liang Y., Zimin A.V., Pertea G., Qi P., Bennetzen J.L.B., Dai X.T., Dawson M.W., Muller H.G., Kugler K., Rivarola-Duarte L., Spannagl M., Mayer K.F.X., Lu F.H., Bevan M.W., Leroy P., Li P.C., You F.M., Sun Q.X., Liu Z.Y., Lyons E., Wicker T., Salzberg S.L., Devos K.M., Dvorak J. (2017): Genome sequence of the progenitor of the wheat D genome *Aegilops tauschii*. Nature, 551: 498–502.

Ma H.X., Bai G.H., Gill B.S., Hart L.P. (2006): Deletion of a chromosome arm altered wheat resistance to Fusarium head blight and deoxynivalenol accumulation in Chinese Spring. Plant Disease, 90: 1545–1549.

Ma Z.Q., Xie Q., Li G.Q., Jia H.Y., Zhou J.Y., Kong Z.X., Li N., Yuan Y. (2020): Germplasms, genetics and genomics for better control of disastrous wheat Fusarium head blight. Theoretical and Applied Genetics, 133: 1541–1568.

McCullagh P. (2019): Generalized Linear Models. 2nd Ed. Boca Raton, Chapman and Hall/CRC.

Miller S.S., Watson E.M., Lazebnik J., Gulden S., Balcerzak M., Fedak G., Ouellet T. (2011): Characterization of an alien source of resistance to Fusarium head blight transferred to Chinese Spring wheat. Botany-Botanique, 89: 301–311.

Rommel R., Jenkins B.C. (1959): Amphiploids in Triticeae produced at the University of Manitoba from March 1958 to December 1959. Wheat Information Service, 9–10: 23.

Rozen S., Skaletsky H.J. (2000): Primer3 on the WWW for general users and for biologist programmers. In: Krawet S., Misener S., Totowa N.J. (eds.): Bioinformatics Methods and Protocols: Methods in Molecular Biology. Humana Press: 365–386.

Schweiger W., Steiner B., Vautrin S., Nussbaumer T., Siegwart G., Zamini M., Jungreithmeier F., Gratl V., Lemmens M., Mayer K.F.X., Bérgès H., Adam G., Buerstmayr H. (2016): Suppressed recombination and unique candidate genes in the divergent haplotype encoding *FHb1*, a major Fusarium head blight resistance locus in wheat. Theoretical and Applied Genetics, 129: 1607–1623.

Sears E.R. (1977): An induced mutant with homoeologous pairing in common wheat. Canadian Journal of Genetics and Cytology, 19: 585–593.

Shen R., Kong L.R., Ohm H. (2004): Fusarium head blight resistance in hexaploid wheat (*Triticum aestivum*)-*Lophopyrum* genetic lines and tagging of the alien chromatin by PCR markers. Theoretical and Applied Genetics, 108: 808–813.

Su Z.Q., Jin S.J., Zhang D.D., Bai G.H. (2018): Development and validation of diagnostic markers for FHB region, a major QTL for head blight resistance in wheat. Theoretical and Applied Genetics, 131: 2371–2380.

Tuleen N.A., Hart G.E. (1988): Isolation and characterization of wheat – *Elytrigia elongata* chromosome 3E and 5E addition and substitution lines. Genome, 30: 519–524.

Waldron B.L., Moreno-Sevilla B., Anderson J.A., Stack R.W., Frohberg R.C. (1999): RFLP mapping of QTL for fusarium head blight resistance in wheat. Crop Science, 39: 805–811.

Wang H., Sun S., Ge W., Zhao L., Hou B., Wang K., Lyu Z., Chen L., Xu S., Guo J., Li M., Su P., Li X., Wang G., Bo C., Fang X., Zhuang W., Cheng X., Wu J., Dong L., Chen W., Li W., Xiao G., Zhao J., Hao Y., Xu Y., Gao Y., Liu W., Liu Y., Yin H., Li J., Li X., Zhao Y., Wang X., Ni F., Ma X., Li A., Xu S.S., Bai G., Nevo E., Gao C., Ohm H., Kong L. (2020): Horizontal gene transfer of *Fhb7* from fungus underlies Fusarium head blight resistance in wheat. Science, 368: eaba5435.

Wang L.S., Zhang Y., Zhang M.Q., Gong D.C., Mei Y.Z., Dai C.C. (2023): Engineered *Phomopsis liquidambaris* with *Fhb1* and *Fhb7* enhances resistance to *Fusarium graminearum* in wheat. Journal of Agricultural and Food Chemistry, 71: 1391–1404.

Xu J.L., Wang L., Deal K.R., Zhu T.T., Ramasamy R.K., Luo M.C., Malvick J., You F.M., McGuire P.E., Dvorak J. (2020): Genome-wide introgression from a bread wheat × *Lophopyrum elongatum* amphiploid into wheat. Theoretical and Applied Genetics, 133: 1227–1241.

Zhang M.Y., Zhang W., Zhu X.W., Sun Q., Yan C.H., Xu S.S., Fiedler J., Cai X.W. (2020): Dissection and physical mapping of wheat chromosome 7B by inducing meiotic recombination with its homoeologues in *Aegilops speltoides* and *Thinopyrum elongatum*. Theoretical and Applied Genetics, 133: 3455–3467.

Zhang W., Cao Y.P., Zhang M.Y., Zhu X.W., Ren S.F., Long Y.M., Gyawali Y., Chao S.M., Xu S., Cai X.W. (2017): Meiotic homoeologous recombination-based alien gene introgression in the genomics era of wheat. Crop Science, 57: 1189–1198.

Zhang W., Zhu X.W., Zhang M.Y., Chao S.M., Xu S., Cai X.W. (2018): Meiotic homoeologous recombination-based mapping of wheat chromosome 2B and its homoeologues in *Aegilops speltoides* and *Thinopyrum elongatum*. Theoretical and Applied Genetics, 131: 2381–2395.

Zhang W., Danilova T., Zhang M.Y., Ren S.F., Zhu X.W., Zhang Q.J., Zhong S.B., Dykes L., Fiedler J., Xu S., Frels K., Wegulo S., Boehm J., Cai X.W. (2022): Cytogenetic and genomic characterization of a novel tall wheatgrass-derived *Fhb7* allele integrated into wheat B genome. Theoretical and Applied Genetics, 135: 4409–4419.

Zhang X.L., Shen X.R., Hao Y.F., Cai J.J., Ohm H.W., Kong L.R. (2011): A genetic map of *Lophopyrum ponticum* chromosome 7E, harboring resistance genes to Fusarium head blight and leaf rust. Theoretical and Applied Genetics, 122: 263–270.

Received: August 29, 2024
Accepted: November 25, 2024
Published online: December 16, 2024